

Optimisation of the Lateral Spot-Size Converter

M. Mjeku and S. Haxha

Photonics Group, Department of Electronics, University of Kent, Canterbury

Abstract- In this paper, the design of the laterally tapered spot size converter (SSC) based on a silicon-on-insulator (SOI) is demonstrated. Optimisation of the fabrication parameters of the SSC has been presented. Full vectorial beam propagation method (BPM) in conjunction with modal solution based on the Finite Element Method (FEM) have been employed to investigate the spot-size area along the device length.

1. INTRODUCTION

Integration of optical components into a single chip like their electronic counterparts remains still a serious challenge in photonics. Substrates such as SOI with a high index wafer promise a reliable and low cost alternative for integration of photonic devices. These are highly confined structures due to the high refractive index difference between the silicon, air and SiO₂, resulting in low loss waveguides and high confinement of the light. Integration of different photonics components into a single wafer requires the optimisation of their fabrication parameters. One of the serious issues in realization of integrated components into a single chip is coupling between different components. Dimensions of these photonic components are different and as a result their spot sizes also differ. Passive components such as electro-optic modulators and optical amplifiers usually have a small and non-symmetrical spot size. SMF have a circular and much larger spot-size diameter in the range of 8-10 μm . In the case when these devices are direct coupled with each other, almost total power would be lost due to their mode mismatch. The mode mismatch issue has been approached in different ways; such as a prism coupler or a micro-lense, and mode transformers. Various waveguide SSCs have been demonstrated in literature [1, 2]. Most of them are based in tapering the waveguide structure laterally, vertically or in both lateral and vertical directions. In this paper we have optimised several key parameters of the laterally tapered waveguide to achieve high coupling efficiency. In this work, the SSC compatible with the electrooptic modulator [3] is presented. The SOI structures can be fabricated by using conventional fabrication techniques. However, it is always necessary to develop accurate models to predict the behaviour of the photonic devices prior to their fabrication. In this study, rigorous numerical techniques such as BPM in conjunction with modal solution based on FEM have been employed to optimise the SSC performance.

2. COMPUTATIONAL TECHNIQUES

In this study rigorous numerical techniques have been employed to investigate the mode shape and their propagation characteristics. The full vectorial H-field mode solver and the vectorial H-field beam propagation method (BPM) are considered amongst the most rigorous full vectorial approaches for the characterisation of optical waveguides [4, 5]. These methods are based on the finite element method (FEM) which considers the cross section of the waveguide as a number of different dimension triangles connected to each other by their vertices. The vectorial beam propagation method used in this work incorporates the nonparaxial wide-angle approach and the perfectly matched layer (PML) boundary condition.

3. RESULTS AND DISCUSSIONS

The SSC structure studied in this paper is shown in Fig. 1. This SSC consists of a silica waveguide core with a refractive index of 1.456 on a SOI substrate. The structure is placed on a thick Si substrate with high refractive index of 3.479. The leakage loss due to the high refractive index substrate can be minimised by optimising the width of the SiO₂ buffer layer. The operation wavelength is 1.55 μm . The optical modes are confined in the silica core. The silica core supports the optical mode until the width of the core is larger than the cut-off width. When the width of the silica waveguide is reduced below the cut-off width, then the silica core does not support the mode any more and the mode expands into the SiO₂ buffer layer which serves as a secondary core. The initial width of the core is 3.5 μm and the height is 6.0 μm . The width and height of the SiO₂ buffer layer are 10 μm and 9.8 μm , respectively, the thickness of the lower guiding layer is set to 0.2 μm . The effect of the final width W_f on the SSC performance has been investigated. Fig. 3 shows the resulting spot-size area of the lateral SSC for a taper length equal to 400 μm and various final widths equal to 0.3 μm , 0.6 μm and 0.8 μm . The spot-size area defined here is the exponential spot-size. It can be seen from the figure that the spot-size decreases linearly when the width is reduced. The mode expansion has occurred only when the final width is 0.3 μm . For

the final width of $0.6\ \mu\text{m}$ and $0.8\ \mu\text{m}$ as shown here with dotted and dashed lines, respectively, the mode expansion has not occurred. It can be observed that the mode conversion has been achieved at $W = 0.5\ \mu\text{m}$. In other words the SSC with the length of $400\ \mu\text{m}$ can be realised only when final width is less than $0.5\ \mu\text{m}$. To investigate the effect of the taper length on the SSC performance, the taper length of $800\ \mu\text{m}$ and $1500\ \mu\text{m}$ are considered. Fig. 4 shows the variation of the spot-size area as a function of the taper width when the taper length of $800\ \mu\text{m}$ and the final widths of $0.3\ \mu\text{m}$, $0.6\ \mu\text{m}$ and $0.8\ \mu\text{m}$ are considered. The evolution of the field profile in three different cross sections of the SSC is shown in Fig. 2. It can be seen that the mode has expanded from one section to another until it settled down at the final width of $0.3\ \mu\text{m}$. For the final width of $0.8\ \mu\text{m}$ the mode has just started to appear into the secondary guide. For the taper length of $800\ \mu\text{m}$ and the final width of $0.8\ \mu\text{m}$ the mode conversion has occurred at $W = 1.0\ \mu\text{m}$. This clearly shows that mode expansion can be realised even at a larger width than 0.5 , however the taper length would be increased. Finally, the taper length of $1500\ \mu\text{m}$ is investigated and presented in Fig.5. It is clear from this figure that the spot-size has expanded and settled into the secondary guide for all the three widths of $0.3\ \mu\text{m}$, $0.6\ \mu\text{m}$ and $0.8\ \mu\text{m}$, shown with solid, dotted and dashed lines, respectively. The SS expansion has occurred at the width of $1.0\ \mu\text{m}$ and the taper length of $1200\ \mu\text{m}$ when the final width of $0.3\ \mu\text{m}$ is considered, as shown in Fig. 6. Our simulations indicate that for a smaller final width the mode expansion occurs at a shorter taper length. From the investigation of the coupling efficiency, we managed to get coupling efficiency higher than 90% when the mode expansion has achieved. The spot-size oscillations shown in the graph are due to the interference between the fundamental mode and the higher order modes. The amplitude of these oscillations continuously reduces with the taper length, as can be seen from this figure, after the first peak, the amplitude has started to reduce.

4. CONCLUSIONS

A silica waveguide spot size converter based on a SOI substrate compatible with an electro-optically clad silica waveguide modulator is reported. Rigorous and accurate numerical simulations based on the vectorial finite element formulations of Maxwell's equations are employed. Optimisation of the structure is carried out by changing different parameters such as the length of the taper and final width. The coupling efficiency has been significantly improved when the mode conversion is achieved. Rigorous simulations show that the interference of the fundamental mode with the higher order modes can be optimised by a careful selection of fabrication parameters.

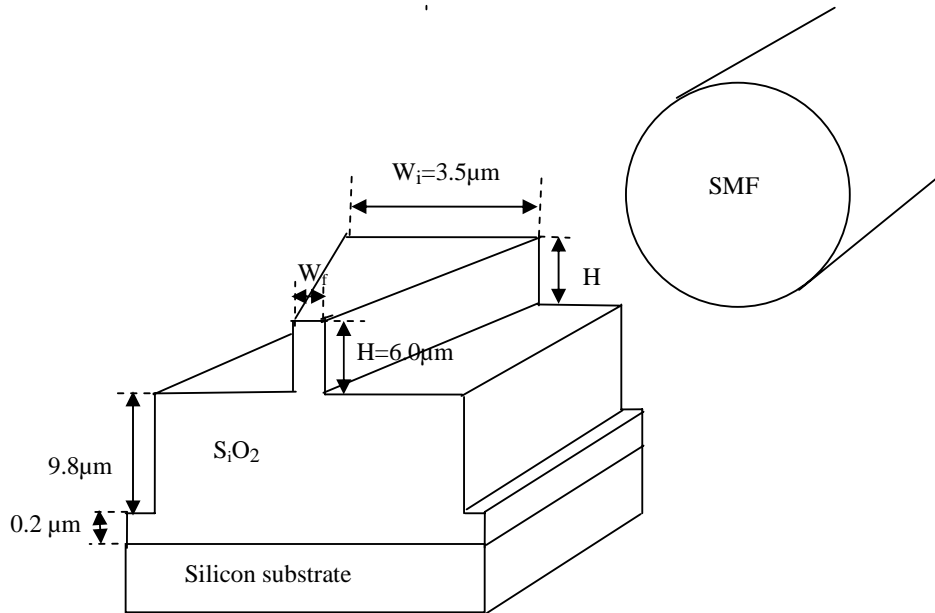


Fig. 1 Schematic diagram of the silica waveguide SSC design

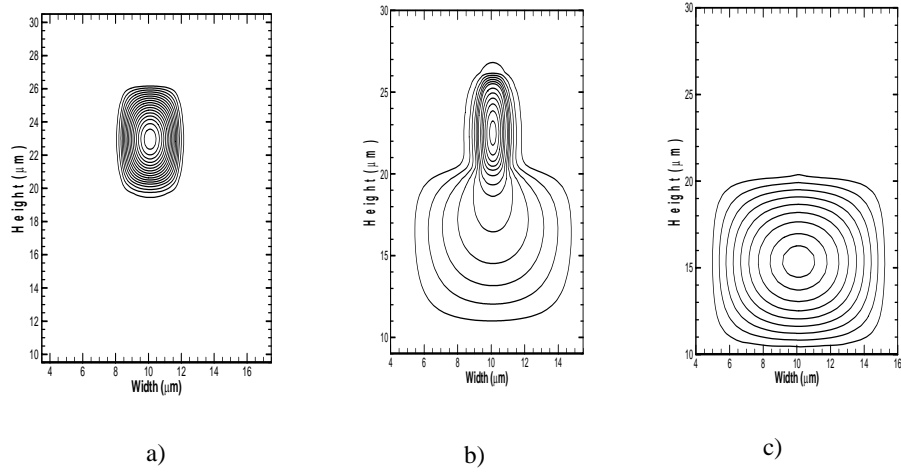


Fig. 2 TE mode profile for a $800\mu\text{m}$ SSC, $W_T=0.3$ a) at the beginning of the taper b) along the taper when $W = 0.8\mu\text{m}$ c) at the end of the taper when the mode has expanded into the second guide.

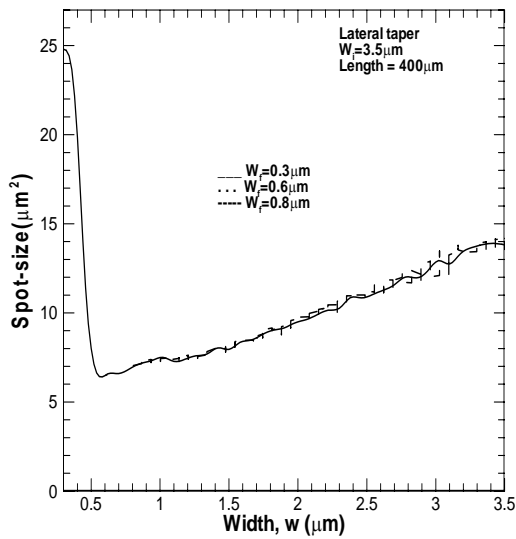


Fig. 3 Variation of spot-size area as a function of the guide width for a taper length of $400\mu\text{m}$ and for final widths equal to $0.3\mu\text{m}$, $0.6\mu\text{m}$ and $0.8\mu\text{m}$

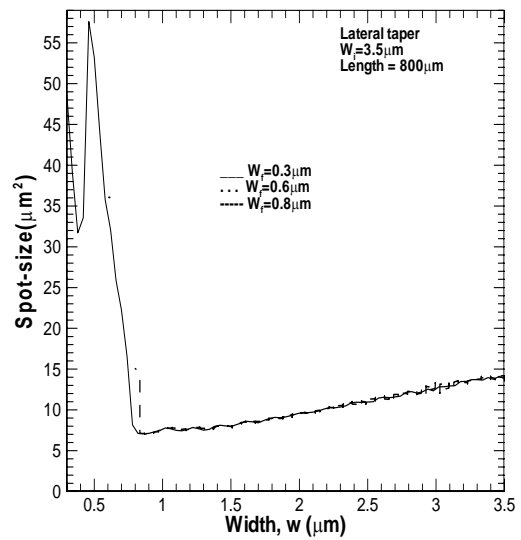


Fig. 4 Variation of spot-size area as a function of the guide width for a taper length of $800\mu\text{m}$ and for final widths equal to $0.3\mu\text{m}$, $0.6\mu\text{m}$ and $0.8\mu\text{m}$

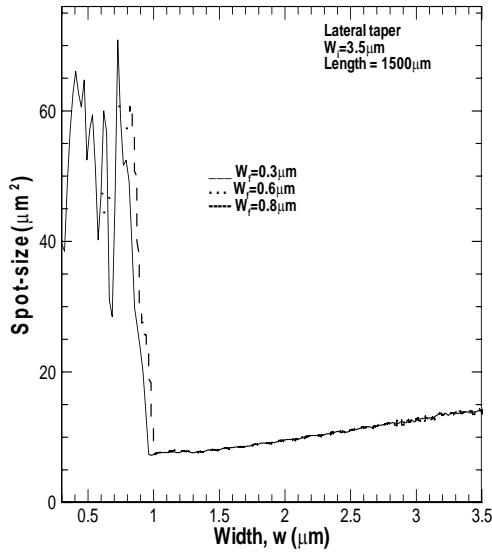


Fig. 5 Variation of spot-size area as a function of the guide width for a taper length of 1500 μm and for final widths equal to 0.3 μm , 0.6 μm and 0.8 μm

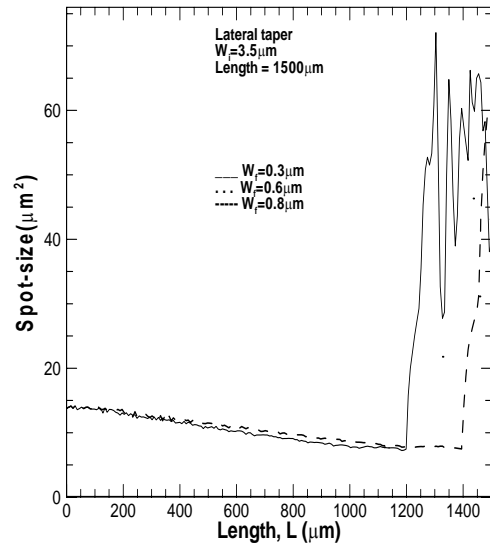


Fig. 6 Variation of spot-size area as a function of the guide length for a taper length of 1500 μm and for final widths equal to 0.3 μm , 0.6 μm and 0.8 μm

REFERENCES

- [1] P. Sewell, T. M. Benson, and P. C. Kendall, "Rib waveguide spot-size transformers: modal properties," *J. Light wave Technol.*, vol. 17, no. 5, pp. 848-856, 1999.
- [2] R. S. Fan, and R. B. Hooker, "Tapered polymer single-mode waveguides for mode transformation," *J. Lightwave Technol.*, vol. 17, no. 3, pp. 466-474, 1999.
- [3] R. Ridgway, D. Nippa, S. Risser, V. McGinniss, "Silica waveguide electrooptic modulator employing push-pull electrodes". *IPR Paper IThC2*, June 2004
- [4] B. M. A. Rahman and S. Haxha, "Optimisation of microwave properties of ultrahigh-speed etched and unetched lithium niobate electrooptic modulators" *J. Lightwave Technol.*, vol. 20, 10, pp. 1856-1862, 2002.
- [5] B. M. A. Rahman, W. Boonthittanont, S. S. A. Obayya, T. Wongcharoen, E. O. Ladele, and K. T. V. Grattan, "Rigorous Beam Propagation Analysis of Tapered Spot-Size Converters in Deep-Etched Semiconductor Waveguides", *J. Lightwave Technol.*, vol. 21, 12, 2003.